J|A|C|S
ARTICLES
Published on Web 05/09/2002

Ozonides, Epoxides, and Oxidoannulenes of C_{70}

Dieter Heymann,*,§ Sergei M. Bachilo,† and R. Bruce Weisman*,†

Contribution from the Department of Earth Science and the Department of Chemistry, Rice Quantum Institute, and Center for Nanoscale Science and Technology, Rice University, Houston, Texas 77251

Received November 6, 2001

Abstract: Six new monoadducts of C_{70} with oxygen species have been prepared, isolated, and characterized following ozonation of C_{70} solutions. The initial products are two ozonide monoadducts, identified as *a,b*- and *c,c*-$C_{70}O_3$. These ozonides lose O_2 through thermolysis or photolysis to form various isomers of $C_{70}O$. The *a,b*-$C_{70}O_3$ isomer dissociates through thermolysis with a decay time of 14 min at 296 K to form the [6,6]-closed epoxide *a,b*-$C_{70}O$. When photolyzed, it instead forms a [5,6]-open oxidoannulene identified as *a,a*-$C_{70}O$. These reactions mimic those seen for $C_{60}O_3$. By contrast, the *c,c*-$C_{70}O_3$ isomer, which has a thermolysis lifetime of 650 min at 296 K, decays thermally only to an oxidoannulene deduced to be *d,d*-$C_{70}O$. Photolysis of *c,c*-$C_{70}O_3$ produces a mixture of the oxidoannulenes *b,c*-$C_{70}O$ and *c,d*-$C_{70}O$ plus a minor amount of the *c,c*-epoxide. All four $C_{70}O$ oxidoannulene isomers undergo photoisomerization, giving eventually the *a,b*- and *c,c*-$C_{70}O$ epoxides.

Introduction

Although C_{70}, the second most abundant fullerene, is similar in many ways to C_{60}, it differs in that its atoms occupy five distinct environments, rather than one. These sites are denoted by the labels *a* through *e* in the partial Schlegel projection of Figure 1. Apical or polar bonds near the C_5 symmetry axis of C_{70} show alternations in bond order similar to those in C_{60}, while the equatorial bonds are more aromatic, with nearly equal orders. The first reported derivative of C_{70} was the oxide $C_{70}O$, isolated from fullerene soot in 1991 by Diederich et al.[1] In subsequent research, C_{70} oxides were synthesized by ozonation and then characterized by HPLC and mass spectrometry.[2−4] Early quantum chemical calculations on $C_{70}O$ suggested that the most stable isomer contains an oxygen bridge across an equatorial ring junction in a "[6,6]-open" structure.[5] In 1996, Smith et al. prepared C_{70} oxides by photooxygenation and obtained the first structural assignments through interpretation of UV−vis and ^{13}C and ^{3}He NMR spectra.[6] These workers found comparable quantities of two [6,6]-closed epoxide isomers in which the oxygen bridged either *a,b* or *c,c* bonds. Bezmelnitsin et al. confirmed this assignment and disentangled the ^{13}C NMR spectra of the two epoxides.[7] Although neither of these groups was able to separate the epoxide isomers from one another, isomeric separation through HPLC was reported by Balch et al. in conjunction with an X-ray structural study.[8] Semiempirical quantum simulations of C_{70} ozonation deduced the *a,b* and *c,c* [6,6]-closed epoxide isomers to be the most probable oxide products.[9,10]

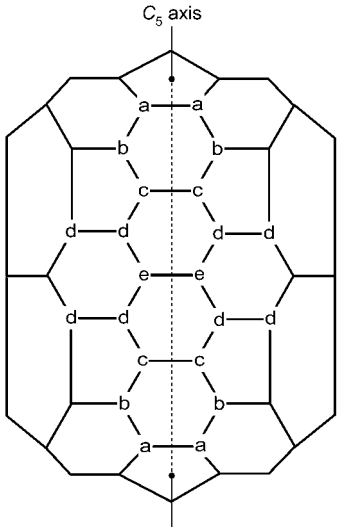

Figure 1. Partial projection of the C_{70} structure, illustrating locations of the five carbon atom sites and the eight types of bonds between adjacent atoms.

* Corresponding author. E-mail: weisman@rice.edu.
§ Department of Earth Science.
† Department of Chemistry.

(1) Diederich, F.; Ettl, R.; Rubin, Y.; Whetten, R. L.; Beck, R.; Alvarez, M. M.; Anz, S. J.; Sensharma, D.; Wudl, F.; Khemani, K. C.; Koch, A. *Science* **1991**, *252*, 548−551.
(2) Heymann, D.; Chibante, L. P. F. *Recl. Trav. Chim. Pays-Bas* **1993**, *112*, 531−534.
(3) van Cleempoel, A.; Gijbels, R.; Claeys, H.; van den Heuvel, H. *Rapid Commun. Mass Spectrom.* **1996**, *10*, 1579−1584.
(4) Heymann, D.; Chibante, L. P. F. *Chem. Phys. Lett.* **1993**, *207*, 339−342.
(5) Raghavachari, K.; Rohlfing, C. M. *Chem. Phys. Lett.* **1992**, *197*, 495−498.
(6) Smith, A. B., III; Strongin, R. M.; Brard, L.; Furst, G. T.; Atkins, J. H.; Romanow, W. J.; Saunders: M.; Jimenez-Vazquez, H. A.; Owens, K. G.; Goldschmidt, R. J. *J. Org. Chem.* **1996**, *61*, 1904−1905.
(7) Bezmelnitsin, V. N.; Eletskii, A. V.; Schepetov, N. G.; Avent, A. G.; Taylor, R. *J. Chem. Soc., Perkin Trans. 2* **1997**, 683−686.
(8) Balch, A. L.; Costa, D. A.; Olmstead, M. M. *Chem. Commun.* **1996**, 2449−2450.
(9) Wang, B.-C.; Chen, L.; Chou, Y.-M. *THEOCHEM* **1998**, *422*, 153−158.
(10) Wang, B.-C.; Chen, L.; Lee, K.-J.; Chen, C.-Y. *THEOCHEM* **1999**, *469*, 127−134.

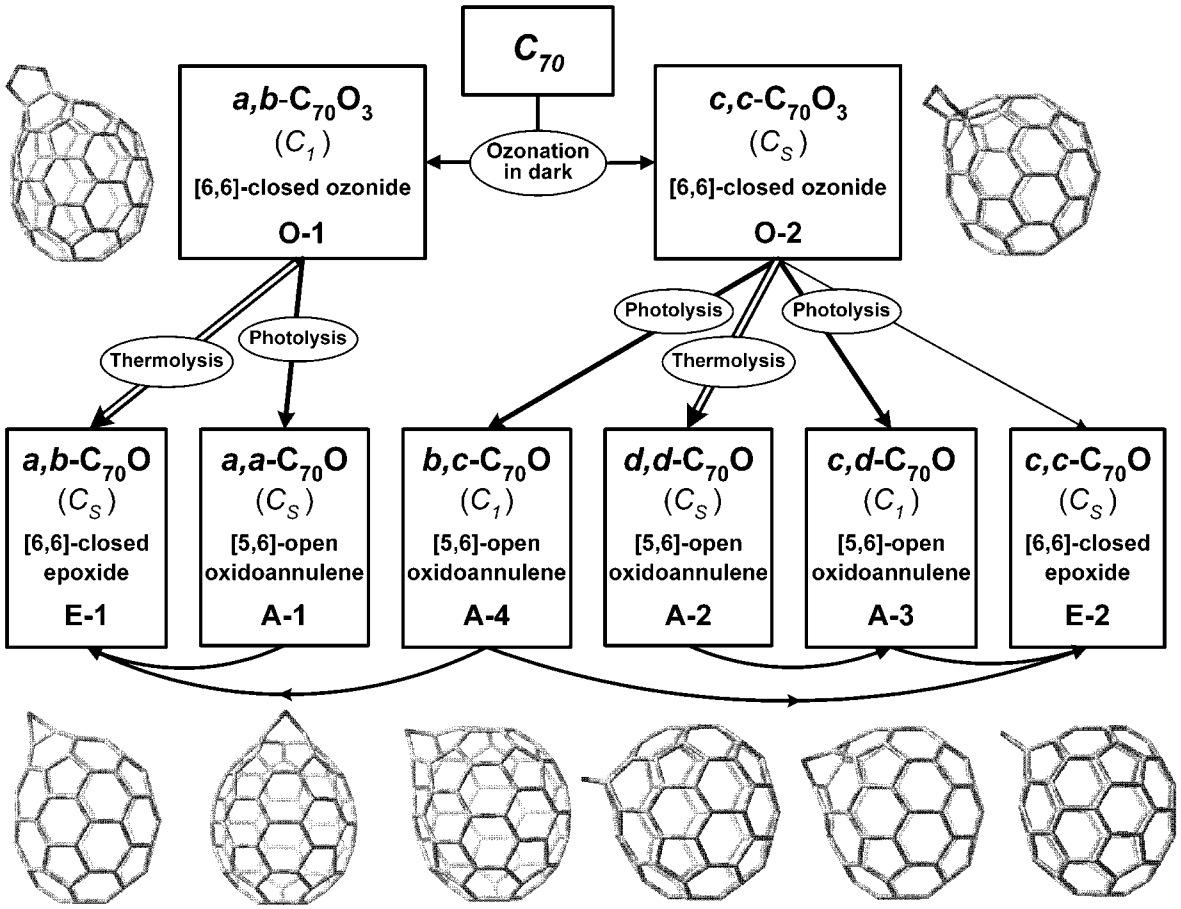

Figure 2. Diagram showing reaction pathways deduced for the ozonide and oxide monoadducts of C_{70} formed through exposure of dissolved C_{70} to ozone. All of the curved arrows connecting $C_{70}O$ isomers represent photoisomerization processes.

New insights into the oxides of C_{60} have recently been reported from this laboratory. We showed that ozonation of C_{60} initially forms the ozone adduct $C_{60}O_3$, which thermally dissociates on the time scale of minutes near room temperature to produce the epoxide $C_{60}O$.[11] Most recently, we found that photolysis of the ozonide $C_{60}O_3$ efficiently forms a new isomer of $C_{60}O$, the [5,6]-open oxidoannulene (oxa-homo[60]fullerene).[12] These findings suggest that the ozonation of C_{70} under controlled conditions may reveal ozonide adducts or new isomers of $C_{70}O$. Whereas there are only two possible isomers of $C_{60}O$ in which the oxygen bridges adjacent carbon atoms, Figure 1 shows that eight such isomers are possible for C_{70}, four bridging [6,6]-junctions and four bridging [5,6]-junctions. A detailed study of C_{70} ozonation may therefore face both the promise and the challenge of separating and identifying multiple isomeric products.

We report here the results of such an ozonation study that has focused exclusively on monoadducts. In the course of this work we have uncovered and characterized two C_{70} ozonide isomers having quite different stabilities and unimolecular reactions. Thermolysis and photolysis of these ozonides leads to the two epoxides reported earlier, plus four previously unknown oxidoannulenes that are analogous to the recently discovered [5,6]-isomer of $C_{60}O$. In all, six of the eight possible isomers of C_{70} have thus been observed. Surprisingly, we find that all four $C_{70}O$ oxidoannulenes undergo photoinduced transformations to other $C_{70}O$ isomers.

Results

Overview. We have previously reported that ozonation of C_{60} produces an unstable intermediate identified as $C_{60}O_3$, the [6,6]-closed ozone adduct of C_{60}.[11] We find that a similar reaction occurs with C_{70}, forming two isomers of $C_{70}O_3$. Like $C_{60}O_3$, each of these C_{70} ozonides loses O_2 through thermolysis or photolysis, giving different isomers of $C_{70}O$ by each route. Ozonation of C_{70} thereby leads to six $C_{70}O$ isomers, of which two are [6,6]-closed epoxides and four are oxidoannulenes analogous to the recently reported [5,6]-open isomer of $C_{60}O$.[12] We have also observed photoisomerization of all of the $C_{70}O$ annulenes. Figure 2 summarizes this complex set of species and processes. In the sections below, we present the spectroscopic, kinetic, and logical evidence used to deduce this scheme.

Ozonide Formation. When a stream of ozone and oxygen was slowly bubbled through a dark, chilled solution of C_{70} in toluene or *o*-xylene, two new unstable adducts were quickly produced. Figure 3 shows an HPLC chromatogram measured with a chilled column immediately after such ozonation of a C_{70} sample. In addition to the peak at 7.8 min from unreacted C_{70}, there are two prominent product peaks at 6.3 and 6.8 min (labeled O-2 and O-1, respectively). Both of these species, which we have identified as ozonide adducts of C_{70}, thermally convert to different C_{70} adducts in darkness. Samples containing only

(11) Heymann, D.; Bachilo, S. M.; Weisman, R. B.; Cataldo, F.; Fokkens, R. H.; Nibbering, N. M. M.; Vis, R. D.; Chibante, L. P. F. *J. Am. Chem. Soc.* **2000**, *122*, 11473−11479.
(12) Weisman, R. B.; Heymann, D.; Bachilo, S. M. *J. Am. Chem. Soc.* **2001**, *123*, 9720−9721.

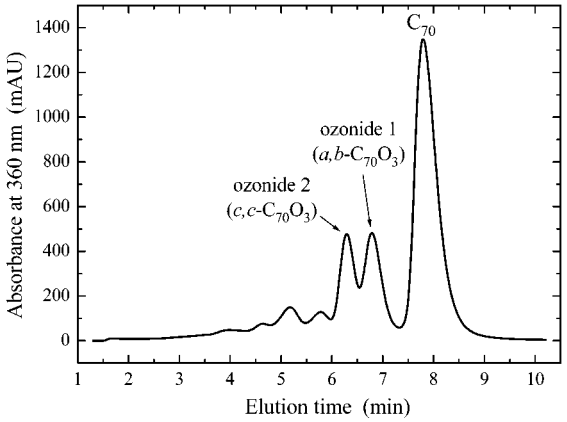

Figure 3. HPLC chromatogram of a sample of C_{70} in *o*-xylene immediately following ozonation at −18 °C. A 4.6 × 250 mm Cosmosil PBB column held at 0 °C was used with toluene eluent flowing at 2 mL min^{-1}. The detection wavelength was 360 nm. Peaks prior to 6 min are assigned to higher ozonides and oxides of C_{70}.

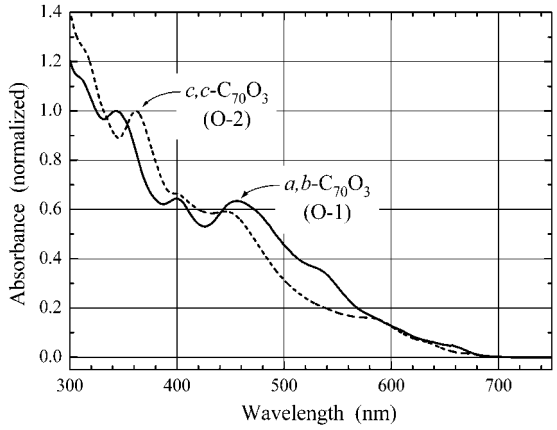

Figure 4. UV−vis absorbance spectra of the two ozonide adducts of C_{70}. O-1 (a,b-$C_{70}O_3$) is shown as a solid curve and O-2 (c,c-$C_{70}O_3$) is shown as a dashed line. For comparison, both spectra have been normalized to 1 at their near-UV peaks.

O-1 were obtained from HPLC separation runs performed on a chilled PBB column immediately after ozonation. To obtain pure samples of O-2, we held the ozonated C_{70} solutions at room temperature for about 1 h, after which the O-1 had almost completely decomposed but nearly all of the O-2 remained for collection as an HPLC fraction. In Figure 4 we present the UV−vis absorption spectra of O-1 and O-2 in toluene solution. O-1 shows characteristic peaks at 343, 399, and 456 nm, and a shoulder at 535 nm, whereas O-2 has peaks at 362, 401, and 445, plus a shoulder near 585 nm.

Products from Ozonide 1. Species O-1 decays thermally to form only one detectable product. As shown in the Supporting Information for this report, the product's ^{13}C NMR spectrum, taken in a $CS_2/CDCl_3$ solvent mixture, shows 35 sp^2 signals at shifts between 130.60 and 153.37 ppm relative to TMS, plus two equal-amplitude sp^3 signals at 92.2 and 90.7 ppm. This is the expected number and pattern of signals for the C_s-symmetry *a,b*-epoxide. Except for small solvent-induced shifts, the positions of these sp^3 signals closely match those reported by Smith et al. and Bezmelnitsin et al. for the *a,b*-isomer of $C_{70}O$ epoxide,[6,7] thereby identifying the thermolysis product as the *a,b*-epoxide. We also note that 33 of the 35 sp^2 signals in our spectrum have chemical shifts in excellent agreement with those

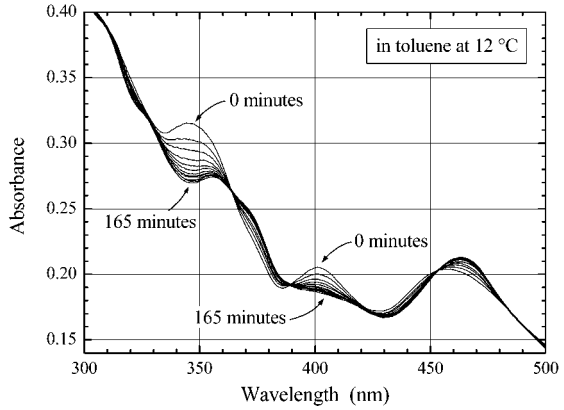

Figure 5. UV−vis absorbance spectra measured during the thermolysis of a,b-$C_{70}O_3$ in toluene at 12 °C.

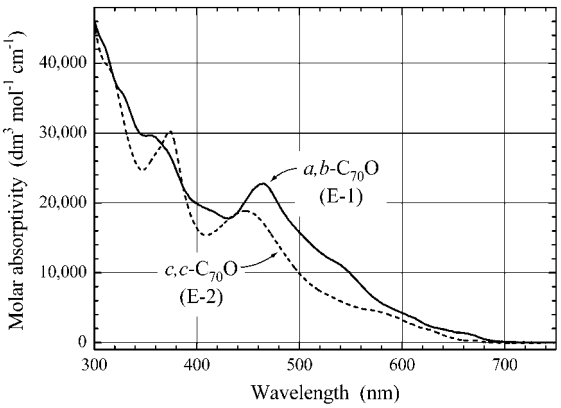

Figure 6. UV−vis absorptivity spectra of the *a,b*- and *c,c*-isomers of $C_{70}O$ epoxide.

deduced by Bezmelnitsin et al. for a,b-$C_{70}O$ in an isomerically mixed sample.[7] However, we observe no signal corresponding to their 144.51 ppm line, and a 148.28 ppm signal assigned in their report to c,c-$C_{70}O$ is in fact present with normal intensity in our a,b-$C_{70}O$ spectrum.

The thermal reaction of O-1 to form a,b-$C_{70}O$ can be quantitatively monitored through UV−vis spectrophotometry, as illustrated in Figure 5. These spectra were recorded at 15 min intervals starting immediately after HPLC collection of the O-1 fraction from an ozonated sample of C_{70}. The sample cell was held at 12 °C. In addition to the sharp isosbestic points evident at 364, 389, and 454 nm, Figure 5 shows near-isosbestic regions near 310, 328, 422, and 487 nm. As can be seen from the spectrum displayed in Figure 6, a,b-$C_{70}O$ formed through thermolysis of O-1 has absorption features at 354, 464, and 670 nm. On kinetic analysis, the evolving UV−vis data shown in Figure 5 revealed a clean first-order reaction. By spectrophotometrically monitoring the transformation of O-1 to a,b-$C_{70}O$ at temperatures ranging from 7 to 25 °C, we were thus able to deduce rate constants that are plotted in Arrhenius form in Figure 7. These data are well fit by a straight line with a slope of −11345 K, corresponding to a thermolysis activation energy of 94.3 kJ mol^{-1}, or 7890 cm^{-1}. The exponential thermolysis lifetime of O-1 in toluene was 14 min at 23 °C.

When exposed to light, species O-1 undergoes an efficient photochemical reaction to give a product different from the epoxide formed by thermolysis. The photoproduct, which we designate A-1, shows a parent peak at *m/z* 856 in MALDI mass spectrometry. Figure 8 displays the UV−vis absorption spectrum

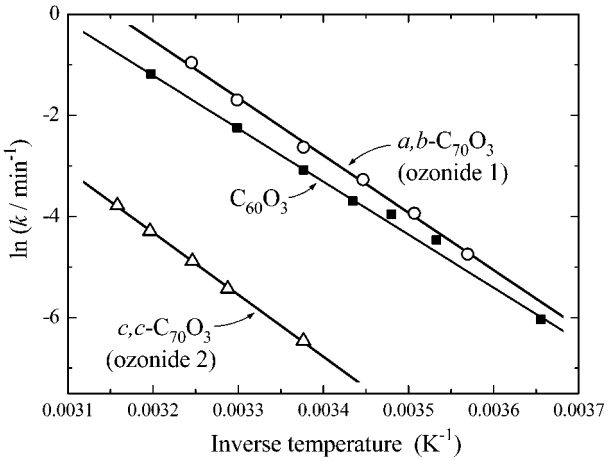

Figure 7. Arrhenius plots for the thermolysis of the *a,b*- and *c,c*-isomers of C_{70} ozonide. Symbols represent measured data points and the solid lines are linear least-squares fits through the data. For comparison, data are also shown for thermolysis of $C_{60}O_3$.

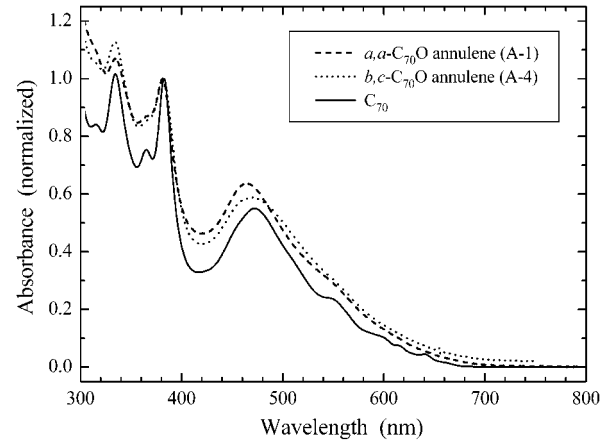

Figure 8. UV−vis absorbance spectra of compounds A-1 (dashed line) and A-4 (dotted line). The spectrum of C_{70} is also plotted (solid line) for comparison. All spectra have been normalized to 1 at the peaks near 382 nm.

of A-1 in room-temperature toluene solution. Peaks are evident at 334.5, 381, and 464 nm. We found that ^{13}C NMR spectroscopy on this compound and others designated A-2, A-3, and A-4 proved very difficult because of their limited solubility and strong tendency to form polymers at the required concentrations. However, using chilled *o*-dichlorobenzene-d_4 as the solvent and a sample isotopically enriched to 4% in ^{13}C, we were able to obtain a weak spectrum of A-1 after 44 h of data acquisition. (see Supporting Information.) No signals were detectable in the chemical shift range expected for sp^3 sites, but approximately 40 signals were observed between 135.33 and 155.49 ppm (relative to TMS). Some of these probably arose from reaction products that were found to have formed during the measurement. We suggest that the singlet at 155.5 ppm, shifted 4.77 ppm further downfield than any other signal, may arise from two equivalent carbons bonded to the oxygen atom.

Products from Ozonide 2. Species O-2, the other primary product of C_{70} ozonation, decays thermally to form a single detectable product that we denote as A-2. Spectrophotometric kinetic data measured for temperatures from 23 to 43.5 °C show that this thermolysis reaction is first order. Compared to thermolysis of O-1, the decay of O-2 is almost 50 times slower,

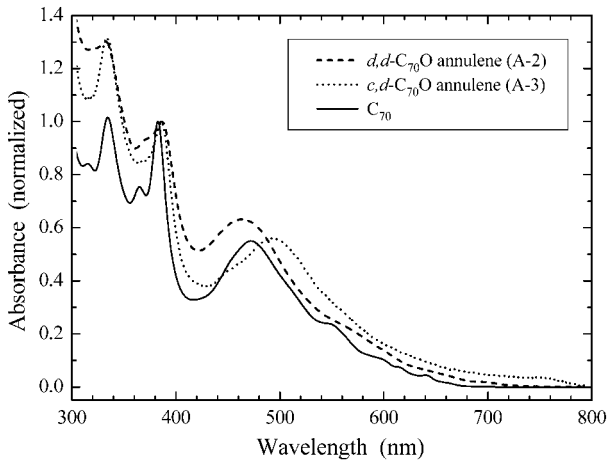

Figure 9. UV−vis absorbance spectra of compounds A-2 (dashed line) and A-3 (dotted line). The spectrum of C_{70} is also plotted (solid line) for comparison. All spectra have been normalized to 1 at the peaks near 383 nm.

with an exponential lifetime of 650 min at 23 °C. Figure 7 shows the measured first-order decay constants in Arrhenius form, along with a linear best fit indicating an activation energy of 102 kJ mol^{-1} (8515 cm^{-1}). The relatively long thermal lifetime of O-2 allowed us to measure its ^{13}C spectrum. For a sample in *o*-dichlorobenzene-d_4 at 5 °C, we found an sp^3 singlet at 97.02 ppm relative to TMS. Such a singlet is consistent with *c,c* but not *a,b* derivatization. We also observed 29 sp^2 signals between 140.65 and 153.86 ppm. The remaining 7 sp^2 signals that would be expected from a C_s-symmetry ozonide are presumably obscured by strong solvent resonances.

MALDI mass spectrometry of A-2, the product of O-2 thermolysis, showed a parent peak at *m/z* 856, as is consistent with the formula $C_{70}O$. In Figure 9 we display the UV−vis absorption spectrum measured for A-2 in toluene. Although MALDI spectra of O-2 gave no peaks above 856, measurements on this compound using the APCI method with a Finnigan MAT 95 mass spectrometer revealed a small but real signal at *m/z* 888, the molecular weight of $C_{70}O_3$. To clarify the O-2 thermolysis reaction, aluminum sample crucibles were filled in the dark with small volumes of O-2 solution and vacuum evaporated to dryness at room temperature. Each crucible, containing approximately 2.5 μg of solid O-2, was then mounted in darkness onto the direct insertion probe of the MAT 95. As the sample crucible was heated, evolved gases were monitored by electron impact ionization at 100 V. The bottom frame of Figure 10 shows a plot of sample temperature as a function of time in this experiment. In the top frame we plot the corresponding ratio of signals measured for O_2 and N_2, along with the results of a control run performed on a similarly prepared sample of C_{70}. The peaks between 100 and 200 s reveal thermolytic production of molecular oxygen from solid O-2.

Species O-2 also decayed photolytically. We irradiated a stirred solution of O-2 in 23 °C toluene with 1.55 mJ, 532 nm pulses from a Q-switched Nd:YAG laser. Samples were withdrawn at selected intervals for HPLC analysis. From the rate of O-2 loss, the irradiation power, the absorptivity at 532 nm, and the cell geometry, we calculated a photochemical quantum yield of 0.09 for this air-saturated sample. The photochemical quantum yield increased to approximately 0.75

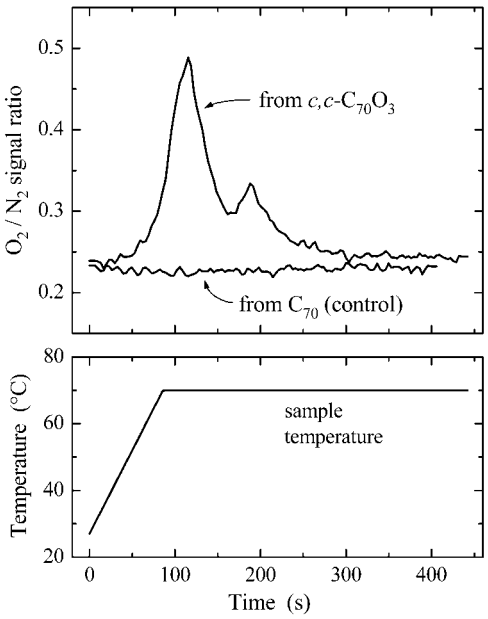

Figure 10. Data collected during thermolysis of a *c,c*-$C_{70}O_3$ (O-2) sample in a mass spectrometer. The bottom frame shows the time-dependent sample temperature during the heating run. The top frame shows the corresponding ratio of ion currents for molecular oxygen and nitrogen evolving from the sample. Also plotted is ion current ratio data for a control sample of C_{70}.

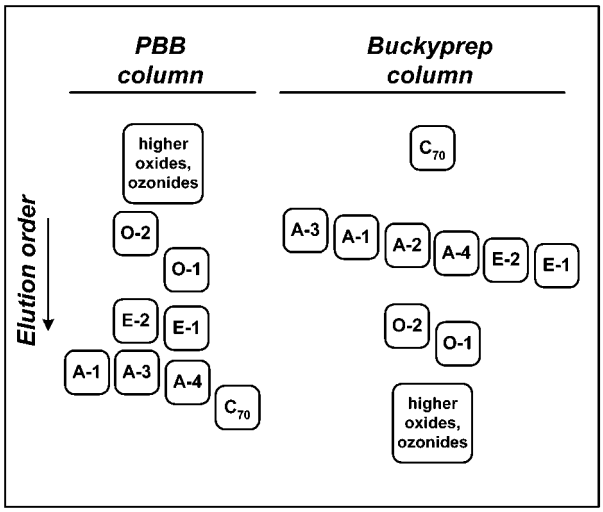

Figure 11. Qualitative illustration of the HPLC elution orders of compounds involved in this study on Cosmosil PBB and Buckyprep columns used with toluene eluent.

when dissolved gases were first removed by freeze−pump−thaw degassing.

In contrast to the behavior of O-1, we found that photolysis of O-2 forms more than one primary photolysis product. A sample of HPLC-purified O-2 was prepared and divided into seven identical 0.53 mL portions, each of which was irradiated for a different duration with 400 nm light from the excitation system of a spectrofluorometer. The irradiated samples were then analyzed using a PBB HPLC column, with the photoproduct fractions collected and reanalyzed on a Buckyprep column. By plotting the HPLC signals from all species as a function of sample irradiation time, we observed smooth decay of the O-2 concentration and increasing concentrations of three new products not detected from O-1 decay. Kinetic analysis showed that the first-order appearance constants for all three products matched the first-order decay constant of O-2. This finding indicates that the three new products are all formed in parallel directly by O-2 photolysis, and that none of them is a secondary photoproduct formed through irradiation of another. We label the major O-2 photoproducts, which appear to be formed in similar amounts, as A-3 and A-4, while the minor photoproduct is called E-2. UV−vis absorption spectra of these compounds are plotted in Figures 9, 8, and 5. In MALDI mass spectrometry, all three show parent peaks at *m*/*z* 856, the value expected for $C_{70}O$.

Judging by its spectrum and stability, we suspected that E-2 was the *c,c*-$C_{70}O$ epoxide previously studied by Smith et al. in mixtures with the *a,b*-$C_{70}O$ epoxide.[6] However, these workers were able to report the UV−vis spectrum only of the isomeric mixture. To spectroscopically confirm the identity of our E-2 species, we repeated the Smith et al. photooxygenation synthesis to obtain a mixture of the two C_{70} epoxides. The individual isomers were then separated from the mixture by repeated HPLC fractionation on a PBB column. We found that the two fractions obtained in this way had UV−vis absorption spectra matching those of our E-1 and E-2 products, shown in Figure 6, thereby confirming that E-2 is indeed the other epoxide isomer, *c,c*-$C_{70}O$. Differences between our epoxide UV−vis data and the spectral peak positions reported previously for the two $C_{70}O$ epoxides may reflect some cross-contamination in the earlier isomeric separation.[8]

Photoisomerization of C_{70} Oxides. We found that the isolation and characterization of species A-1, A-2, A-3, and A-4 was difficult because they are all unstable in the presence of light. By using HPLC to prepare pure samples of these species and then performing controlled irradiations followed by HPLC analyses, we were able to trace the interconversion pathways. These processes are shown as curved lines connecting the bottoms of the boxes in Figure 2. A-2 photoconverts to A-3 with very high efficiency, and A-3 more slowly photoconverts to E-2. When irradiated, compound A-1 converts to E-1. Finally, A-4 appears unique in this set because when exposed to light it directly forms a mixture of two products, E-1 and E-2 (in similar amounts). As discussed below, evidence indicates that all of the A and E compounds have the formula $C_{70}O$. These light-induced transformations should therefore be classified as photoisomerizations. Note that we detected no production of C_{70} in any of the thermal or photoinduced reactions reported here.

Discussion

Isolating the eight oxides and ozonides of C_{70} shown in Figure 2 required a combination of methods. One essential technique was kinetic separation based on the widely differing thermolysis rate constants of ozonides O-1 and O-2. We exploited this difference to simplify the isolation of O-2. By holding ozonated C_{70} solutions at room temperature for about 1 h, the O-1 almost completely thermolyzed to epoxide E-1 while nearly all of the O-2 remained. As can be seen from the qualitative chart of HPLC elution orders in Figure 11, use of a Buckyprep column allowed clean separation of O-2, E-1, and residual C_{70} fractions. Because of its short thermolysis lifetime, O-1 could be isolated from ozonated samples only by prompt HPLC runs on a chilled PBB column. Thermolysis of purified O-1 provided the E-1 epoxide free of the E-2 isomer, whereas photolysis of O-1 gave

A-1. Product A-2 was readily formed through thermolysis of pure O-2. Photolysis of O-2 gave a mixture of A-3, A-4, and E-2. HPLC separations in the dark on a PBB column allowed the epoxides to be well separated from the annulenes, but the A-4 and A-3 fractions overlapped. Pure A-3 samples were most easily prepared by dark thermolysis of O-2 to A-2, followed by efficient photoisomerization to A-3. A final PBB run permitted removal of any E-2 secondary photoproduct.

The results described above reveal a surprising number of compounds whose structures must be deduced. Species O-1 and O-2 have properties strongly suggesting that they are [6,6]-closed adducts of ozone with C_{70}. They are formed in the same way and at comparable rates as [6,6]-closed $C_{60}O_3$ is formed from C_{60} plus ozone. Like $C_{60}O_3$, they readily undergo both thermolysis and photolysis. Moreover, APCI mass spectrometry shows that O-2 has a molecular weight of 888. It loses O_2 in thermolysis to form a compound that has a molecular weight of 856 and photoconverts (through A-3) to *c,c*-$C_{70}O$ (E-2). These observations plus the sp^3 singlet signal in its ^{13}C NMR spectrum indicate that O-2 is the ozonide adduct *c,c*-$C_{70}O_3$. Species O-1 thermolyzes to form only *a,b*-$C_{70}O$ epoxide (E-1) in a process that is seen from Figure 6 to be kinetically very similar to the formation of $C_{60}O$ epoxide from the [6,6]-closed ozonide adduct $C_{60}O_3$. We therefore identify O-1 as *a,b*-$C_{70}O$, the other expected [6,6]-closed ozonide adduct of C_{70}. As was described in the Results section, we identify compounds E-1 and E-2 as two [6,6]-closed epoxide isomers bridging *a,b* and *c,c* bonds, respectively.

Structural assignments for compounds A-1, A-2, A-3, and A-4 begin with the recognition of similarities in their UV−vis absorption spectra. C_{70} has eight chemically distinct sets of C−C bonds: four at the fusions of six-membered rings, and four more at fusions of five- and six-membered rings. Near the poles of C_{70}, the [6,6] bonds have significant double bond character, so derivatization at such bonds essentially removes 2 of the 70 electrons in the parent π system, leaving a single bond between the sp^3-hybridized cage carbon atoms. By contrast, derivatization at the longer [5,6] bonds forms a homofullerene, breaking the underlying cage bond but retaining 70 π-electrons. Consistent with this model, Smith et al. have shown that the [5,6]-open CH_2 derivative of C_{70} (unlike the [6,6]-closed isomer) has a UV−vis absorption spectrum resembling that of pristine C_{70}, particularly near the characteristic 334 and 383 nm peaks.[13] Figures 8 and 9 illustrate that the spectra of A-1, A-2, A-3, and A-4 all share this clear resemblance to C_{70}. As can be seen from the figures or from spectral data tabulated in Table 1, these four compounds have UV peaks at 334.5, 332.5, 333.5, and 334 nm, respectively, as well as at 381, 386.5, 385.5, and 382 nm. These spectral signatures let us identify A-1 through A-4 as [5,6]-open oxidoannulene isomers of $C_{70}O$.

It is then necessary to identify which of the four possible [5,6] derivatization sites in C_{70} (*a,a*; *b,c*; *c,d*; or *d,d*) corresponds to each of the oxidoannulenes A-1 through A-4. We observe that isomer A-1 is unique in that it is formed only from the *a,b*-ozonide, and that it photoisomerizes only to the *a,b*-epoxide. In addition, its NMR spectrum suggests that the oxygen atom is bound to chemically equivalent sites. The only plausible assignment for A-1 is therefore *a,a*-$C_{70}O$. Isomer A-4 is produced from photolysis of *c,c*-$C_{70}O_3$. When exposed to further irradiation, it forms two primary products in comparable yields: the *a,b*- and *c,c*-epoxides. This photoisomerization behavior indicates derivatization adjacent to both the *a,b* and *c,c* bonds. We thereby identify A-4 as *b,c*-$C_{70}O$. According to these assignments, A-1 and A-4 are the two oxidoannulene isomers with the oxygen atom lying nearest to the pole of C_{70}, where bond length alternation is strongest. From this one would expect that the C_{70} π-electron system is less perturbed in A-1 and A-4 than in the more equatorial oxidoannulenes, because the derivatized bonds have less π-character. We note that the absorption spectra shown in Figures 8 and 9 support this view, as A-1 and A-4 show ultraviolet spectra most similar to that of pristine C_{70}.

Table 1. UV−Vis Peak Positions (in toluene solution) for Species Shown in Figure 2

compound	label	absorption maxima (nm)					
C_{70}		334	365	383	472	550 (sh)	640
a,b-$C_{70}O_3$	O-1	343		399	456	535 (sh)	660 (sh)
c,c-$C_{70}O_3$	O-2	362		401	445	585 (sh)	675 (sh)
a,b-$C_{70}O$	E-1	328 (sh)	354		464	540 (sh)	670 (sh)
c,c-$C_{70}O$	E-2		374		448	580 (sh)	670 (sh)
a,a-$C_{70}O$	A-1	334.5	364 (sh)	381	464	550 (sh)	670 (sh)
d,d-$C_{70}O$	A-2	332.5		386.5	463	575 (sh)	700 (sh)
c,d-$C_{70}O$	A-3	333.5		385.5	493		760 (sh)
b,c-$C_{70}O$	A-4	334		382	470		

It now remains to assign A-2 and A-3 to the possible structures *d,d*-$C_{70}O$ and *c,d*-$C_{70}O$. Our key observation is that A-3 photoisomerizes directly to give the *c,c*-epoxide, whereas A-2 photoisomerizes first to A-3 and then from A-3 to the *c,c*-epoxide. Because the *c,c*-epoxide can be formed from *c,d*-$C_{70}O$ by migration of a single C−O bond, but from *d,d*-$C_{70}O$ only by two sequential C−O bond migrations, we assign A-2 to *d,d*-$C_{70}O$ and A-3 to *c,d*-$C_{70}O$. Combined with our experimental findings, this assignment implies that photolysis of O-2, the *c,c*-ozonide, generates similar amounts of *b,c*- and *c,d*-$C_{70}O$ as the main primary products, plus a smaller amount of the *c,c*-epoxide. To rationalize such multiple product formation, one can imagine that photolytic O_2 loss from the *c,c*-ozonide will leave a radical intermediate in which the remaining oxygen atom is bound to one original *c* site. It can then re-bond to neighboring *b* or *d* sites at comparable rates, or to the *c* site at a lower rate.

An intriguing finding is the low yield of direct *c,c*-$C_{70}O$ formation through either photolysis or thermolysis. Although room-temperature thermolysis of *c,c*-$C_{70}O_3$ is ca. 50 times slower than thermolysis of the *a,b*-ozonide, the yield of *c,c*-$C_{70}O$ epoxide is undetectably low (<1%). Thermal dissociation of *c,c*-$C_{70}O_3$ therefore produces the corresponding *c,c*-epoxide at a rate at least 5000 times lower than *a,b*-$C_{70}O_3$ forms the *a,b*-epoxide. The only detected product of *c,c*-$C_{70}O_3$ thermolysis is instead (surprisingly) the *d,d*-$C_{70}O$ annulene. It remains to be understood what features of the potential energy surface inhibit thermal formation of *c,c*-epoxide while allowing formation of *d,d*-$C_{70}O$ annulene. In contrast to thermolysis, photolysis of *c,c*-$C_{70}O_3$ does generate the *c,c*-$C_{70}O$ epoxide, but only as a minor primary product with a relative yield near 10%.

We also note the apparent absence of *e,e*-$C_{70}O$, which is theoretically predicted to be the most stable isomer. This absence probably reflects the higher reactivity of the *a,b* and *c,c* sites to

(13) Smith, A. B.; Strongin, R. M.; Brard, L.; Furst, G. T.; Romanow, W. J.; Owens, K. G.; Goldschmidt, R. J.; King, R. C. *J. Am. Chem. Soc.* **1995**, *117*, 5492−5502.

ozone attack, leaving no kinetically competitive pathway for generating *e*,*e*-$C_{70}O$. Preferential formation of *a*,*b*-C_{70} adducts has been observed in other reactions and sometimes explained in terms of the higher local curvature near the C_{70} pole,[14−16] although addition at the *c*,*c* and other sites is also found for strong reagents and conditions.[6,7,17] It is interesting that photolysis of the *a*,*b*-ozonide selectively produces the *a*,*a*- but not the *b*,*c*-oxidoannulene, whereas photolysis of the *c*,*c*-ozonide produces similar quantities of both adjacent oxidoannulenes, the *b*,*c* and *c*,*d* isomers. We also observe that *d*,*d*-$C_{70}O$ photoisomerizes very efficiently to the *c*,*d*-oxidoannulene, but not to the [6,6]-adducts *d*,*e*-$C_{70}O$ or *e*,*e*-$C_{70}O$. Subsequent photoisomerization of *c*,*d*-oxidoannulene to the *c*,*c*-epoxide occurs with a much lower quantum yield. Further studies will be needed to clarify the mechanisms of these photochemical reactions and to confirm the deduced structures.

Conclusions

Our results show that the family of monoadducts formed following reaction of C_{70} with ozone is far larger and more reactive than had been known from prior research. This group of compounds can be successfully studied only after recognizing that many of them are unstable in the presence of light, and that others are short-lived even in darkness. The newly observed compounds are identified as two ozonide adducts (*a*,*b*- and *c*,*c*-$C_{70}O_3$) and all four of the possible [5,6]-oxidoannulenes (*a*,*a*-, *b*,*c*-, *c*,*d*-, and *d*,*d*-$C_{70}O$). In addition, we have devised a kinetic method to isolate two epoxides (*a*,*b*- and *c*,*c*-$C_{70}O$) that are otherwise quite difficult to separate.

We find that the *a*,*b*-isomer of $C_{70}O_3$ resembles $C_{60}O_3$ in its unimolecular reactions, forming an epoxide through thermolysis and an oxidoannulene through photolysis. Our results show that dissociation pathways of *c*,*c*-$C_{70}O_3$ differ greatly from those of the *a*,*b*-isomer. Photolysis of *c*,*c*-$C_{70}O_3$ produces mainly two oxidoannulenes, whereas thermolysis gives a different oxidoannulene, deduced to be *d*,*d*-$C_{70}O$. We also observe that *d*,*d*-$C_{70}O$ very efficiently photoisomerizes to form *c*,*d*-$C_{70}O$, another oxidoannulene, and that this product and the other two oxidoannulenes photoisomerize with lower efficiency into $C_{70}O$ epoxides. In the presence of light, therefore, the only stable monoadducts formed after ozonating C_{70} are the two epoxides, *a*,*b*-$C_{70}O$ and *c*,*c*-$C_{70}O$.

Our findings of facile photoisomerizations among C_{70} oxides are surprising and intriguing. The mechanisms of these selective transformations, and of the dissociations of C_{70} ozonides, will likely be understood through further photophysical measurements combined with quantum chemical calculations of ground and lowest triplet state potential surfaces. Such studies are currently in progress. From a synthetic standpoint, the C_{70} oxidoannulenes reported here appear to be unusually reactive species that may find use in new fullerene derivatization schemes. The oxidoannulenes are also promising starting compounds for fullerene oligomerization and polymerization. In view of this synthetic and mechanistic novelty, it seems likely that further study of the C_{70} ozonides and oxidoannulenes will prove very fruitful.

Experimental Methods

Ozonation was performed by bubbling a gas stream of 1 to 2% O_3 in O_2 through sample solutions containing 5 mM C_{70} (99% purity) dissolved in toluene or *o*-xylene. The 1 mL samples were held near −18 °C in darkness while they were exposed to approximately 10^{-5} mol of O_3 over a period of 2 min. Ozone was produced from O_2 using a high-frequency corona discharge generator (Ozone Services model GE60).

HPLC was used extensively for analysis and for preparation of purified compounds. We used Cosmosil Buckyprep, PYE, and PBB columns with toluene as the mobile phase in a Shimadzu system employing a model SPD-M10Avp photodiode array detector. The columns were cooled to 0 °C in an ice bath when analyzing thermally unstable compounds.

Samples of O-1 were obtained from ozonated C_{70} samples by HPLC separation on a chilled 10 mm × 250 mm PBB column immediately after ozonation. We collected pure fractions of O-2 from HPLC runs on samples that had been held at room temperature for approximately 1 h after ozonation.

UV−vis absorption spectra were measured with 1 nm spectral resolution and 0.33 nm point spacing on a Cary 400 spectrophotometer. Sample solutions and reference solvents used in spectrophotometric kinetic runs were held in jacketed cells that were temperature controlled to 0.1 °C with a circulating water bath. For measurement of photochemical quantum yields, we irradiated samples using the excitation system of a Spex Fluorolog 3-21 spectrofluorometer. Routine photolyses were performed using an incandescent illuminator or an ordinary fluorescent lamp.

Three forms of mass spectrometry were applied in this project. Laser desorption time-of-flight spectra measured with a Bruker Biflex III instrument revealed parent peaks used to confirm the formulas of all isolated $C_{70}O$ isomers. A Finnigan MAT 95 instrument operated in APCI mode was used to observe the parent peak of the $C_{70}O_3$ isomer designated O-2. Finally, the Finnigan MAT 95 was operated in electron impact ionization mode with a direct insertion probe to monitor the release of O_2 during thermolysis of compound O-2.

We measured ^{13}C NMR spectra on a Bruker Avance500 spectrometer with samples having either natural abundance (1.1%) or enriched (4% or ca. 15%) ^{13}C contents. Solvents used for the NMR measurements were $CS_2/CDCl_3$ mixtures, *o*-dichlorobenzene-d_4, or toluene-d_8. Cr(acac)$_3$ was added as a spin relaxant.

Acknowledgment. This research has been supported by the National Science Foundation (grant CHE-9900417) and the Robert A. Welch Foundation. We are also grateful to Drs. Larry Alemany and Terry Marriott for their expert advice and patient assistance in NMR and mass spectrometry.

Supporting Information Available: ^{13}C NMR spectra of E-1, O-2, and A-1 (PDF). This material is available free of charge via the Internet at http://pubs.acs.org.

JA012488P

(14) Haddon, R. C. *Science* **1993**, *261*, 1545−1550.
(15) Henderson, C. C.; Rohlfing, C. M.; Gillen, K. T.; Cahill, P. A. *Science* **1994**, *264*, 397−399.
(16) Balch, A. L.; Catalano, V. J.; Lee, J. W.; Olmstead, M. M.; Parkin, S. R. *J. Am. Chem. Soc.* **1991**, *113*, 8953−8955.
(17) Meier, M. S.; Wang, G.-W.; Haddon, R. C.; Brock, C. P.; Lloyd, M. A.; Selegue, J. P. *J. Am. Chem. Soc.* **1998**, *120*, 2337−2342.